Journal of
Computer Science & Systems Biology

Salleh et al., J Comput Sci Syst Biol 2012, 5:2
DOI: 10.4172/jcsb.1000088

Research Article Open Access

The Role of Arg157Ser in Improving the Compactness and Stability of ARM Lipase

Abu Bakar Salleh[1]*, Arilla Sri Masayu Abd Rahim[1], Raja Noor Zaliha Raja Abdul Rahman[2], Thean Chor Leow[3] and Mahiran Basri[4]

[1]*Department of Biochemistry, Faculty of Biotechnology and Biomolecular Sciences, Universiti Putra Malaysia, Serdang, Selangor, Malaysia*
[2]*Department of Microbiology, Faculty of Biotechnology and Biomolecular Sciences, Universiti Putra Malaysia, Serdang, Selangor, Malaysia*
[3]*Department of Cell Biology, Faculty of Biotechnology and Biomolecular Sciences, Universiti Putra Malaysia, Serdang, Selangor, Malaysia*
[4]*Department of Chemistry, Faculty of Sciences, Universiti Putra Malaysia, Serdang, Selangor, Malaysia*

Abstract

Consensus approach is an efficient strategy to identify hot residue important for compactness and stability of protein. Structure of ARM lipase was modeled to explore the possible effect of critical point mutation towards structure and function. The significant difference of amino acid at position 157 between ARM lipase (Arg157) and other thermostable lipases (Ser157) was targeted as a critical residue. Using YASARA software, Arg157 was substituted to Ser and subsequently the energy minimized. Both ARM and R157S lipases were analyzed by MD simulations at different temperatures (50ºC,60ºC, and 70ºC). MD simulation result showed that R157S lipase had lower value of RMSD, RMSF, solvent accessible surface area (SASA) and radius of gyration than native ARM lipase. It indicated that R157S lipase had higher compactness in the structure leading to enhanced stability. To validate the computational data, the substitution of Arg157 to Ser has been conducted using site-directed mutagenesis experimentally. The catalytic efficiency (k_{cat}/K_M) of R157S lipase was refold better than ARM lipase of 70°C. Circular dichorism study revealed that R157S lipase had increased thermostability with higher T_m value (71.6°C) than its wild-type (63.9°C) indicating a better compactness as revealed by spectrofluorocence study. Thus the rational design of substituting Arg157 with Ser improved the protein folding of mutant lipase as shown in MD simulations and subsequently increased the catalytic effectiveness and thermodynamic stability.

Keywords: *Geobacillus sp*; Thermostable lipase; MD simulations; Kinetic study; CD spectra

Abbreviations: K: Kelvin; °C: Degree Celcius; kcat: Rate constant of the enzyme; KM: Affinity of the enzyme for substrate; Vmax: Maximum reaction rate; mdeg: milidegrees; Tm: Melting temperature; λmax: Wavelength maxima; Å:Amstrong; Å2: Amstrong Square; 3D: Three dimensional; MD: Molecular Dynamic; RMSD: Root Mean Square Deviation; RMSF: Root Mean Square Fluctuation; SASA: Accessible Surface Area; SDS-PAGE: Sodium dodecyl sulphate-polyacrylamide gel electrophoresis

Introduction

Thermostable lipases are gaining wide industrial and biotechnological interest due to the fact that they are better suited for harsh industrial processes [1]. Most of thermostable lipases are evolved in thermophilic (growth at temperature above 60°C) and hyperthermophilic (growth at temperatures above 80°C) microbes. The structural comparison between thermolabile and thermostable enzymes has validated the numerous protein stabilizing mechanisms such as hydrophobic interactions, packing efficiency, salt bridges, hydrogen bonds, loop and helix stabilization, reduction of conformational strains and resistance to covalent destruction. On the other hand, the packing of protein atoms is one of the factors in determining thermostability. The higher stability of thermostable enzymes may be contributed by better packing and less internal cavities [2-5].

The principles of protein folding and packing become growing interest to explore how proteins adapt at high temperatures. Protein folding strictly depends on the amino acid sequence of the polypeptide chain. The folding of polypeptide chain is driven by the strong tendency of hydrophobic side chains to cluster in the core of protein away from solvents and stabilized by various non-covalent interactions. The questions are how proteins can have a great variety of functions and specificities when only 20 amino acids are used in their construction and how three dimensional proteins can correspond to their function and specificity. It has been reported that the conformation and stabilization of proteins was due to the properties of amino acid side chains [4,6,7].

Understanding the mechanism of protein folding is crucial and challenging. To realize the goal, rational design has been used to engineer enzyme to create subtle changes by single amino acid substitutions. A novel activity may be obtained with only a single point mutation [8,9]. In this study, consensus approach has been chosen as a simple strategy to identify a critical residue that destabilizes protein structure. The design of stabilizing mutations through consensus approach was proven to be simple and reliable [10]. In the present investigation, recombinant ARM lipase from a newly isolated *Geobacillus sp*. was used [11]. ARM lipase has comparatively low thermostability compared to other homologous thermostable lipases despite sharing a high similarity in amino acid sequences (~80%). The Arg157 has been identified as critical residue that destabilized protein structure. We hypothesized that by substituting Arg157 to Ser would contribute to protein stability because consensus residue fitting well

***Corresponding author:** Abu Bakar Salleh, Department of Biochemistry, Faculty of Biotechnology and Biomolecular Sciences, Universiti Putra Malaysia, Serdang, Selangor, Malaysia, Tel. +603-89466695; Fax +603-89430913; E-mail: abubakar@biotech.upm.edu.my

Received December 23, 2011; **Accepted** April 05, 2012; **Published** April 09, 2012

Citation: Salleh AB, Abd Rahim ASM, Abdul Rahman RNZR, Leow TC, Basri M (2012) The Role of Arg157Ser in Improving the Compactness and Stability of ARM Lipase. J Comput Sci Syst Biol 5: 039-046. doi:10.4172/jcsb.1000088

during evolution. The substitution of critical residue was analyzed using in silico to avoid unnecessary conformational distortion in engineered lipase and validate with kinetic study and thermodynamic study.

Methods

Preparation of 3D structures of ARM and R157S lipases

The 3D structure of ARM lipase was predicted by comparative modeling. The first step in comparative modeling is the assignment of the unknown ARM lipase structure to a protein family with thousands of sequences already stored in protein databases (PDB). The structure of ARM lipase was modeled using available software packages such as HOMOLOGY and MODELLER, Accelrys, San Diego (http://www.accelrys.com). The unknown ARM lipase structure (target protein) was built from the known 3D structure of T1 lipase (2DSN) as a template. The final model of ARM lipase was evaluated using Ramachandran plot. Using YASARA, the three-dimensional structure of the mutant (R157S lipase) was modeled by substituting Arg157 to Ser and energy minimization was used to release bad contact.

MD simulations of ARM and R157S lipases

MD simulations were performed on ARM lipase and R157S lipase structures using Amber03 force field in YASARA package. The periodic box was filled with explicit water molecules to a density of 0.98320 g/l. The whole system was neutralized by adding counter ions and all ionizable protein groups were protonated according to their tabulated pKa values at pH 7 of the medium. Water molecules were relaxed by simulated annealing procedure. Minimization was run until the maximum atom speed dropped below 2200 m/s. Then, the system was heated from 0 to 323 K, 333K and 343 K. Finally, 10,000 ps molecular dynamics (MD) equilibrated simulation were conducted at 323 K, 333 K and 343 K and constant pressure. The cut-off was 7.86 Å for van der Waals interactions. The electrostatic interactions were calculated and 3000 snapshots were collected every 7.5 ps [12]. Analysis of data was done with YASARA and presented as Root Mean Standard Deviation (RMSD), Root Mean Square Fluctuation (RMSF), Solvent Accessible Surface Area (SASA) and radius of gyration.

Organism

The recombinant plasmid pTrcHis/ARM harboring ARM lipase gene was extracted from *Escherichia coli* Top 10 (pTrcHis/ARM) [11] cloned previously grew on Luria-Bertani (LB) agar containing 50 µg/ml ampicillin.

Substitution of Arg157 residue by Site-Directed Mutagenesis

The QuikChange Lightning Site-Directed Mutagenesis Kit (Stratagene, La Jolla, CA, USA) was used as a method to introduce point mutation following the supplier's protocol. The mutagenic primer was designed with centre of mutation position with ~10-15 bases acting as template complementary sequence on both sides. Then, 2µl *Dpn* I restriction endonuclease was added to each amplification reaction to digest the parental methylated DNA. The *Dpn* I-digested DNA was transformed into competent *E. coli* XL-10 Gold cells, and transformants were obtained from LB agar. Each mutation was confirmed by sequencing. Then, confirmed mutant plasmid was transformed into *E. coli* Top 10.

Preparation of crude enzyme solutions of ARM and R157S lipases

The LB broth (200 ml in 1L blue cap bottle) containing 100 µg/ml ampicillin was inoculated with 1 ml of an overnight recombinant culture and incubated at 37°C on a shaking incubator at 200 rpm. The recombinant culture was then induced with 1mM of IPTG. After 17 h of IPTG induction, cells were harvested by centrifugation (10,000 rpm, 4°C, and 10 min). The cell pellets were resuspended with 20 ml of 50 mM phosphate buffer (pH 7.0) and disrupted at 60 W output for 4 min on ice. The supernatants (crude) of ARM and R157S lipases were used in purification.

Purification of ARM and R157S lipases

Purification of ARM and R157S lipases were performed using AKTA Prime using affinity chromatography technique. Four hundred ml culture of ARM and R157S lipases were harvested by centrifugation and resuspended with 40 ml of binding buffer (50 mM phosphate buffer pH 7.4, 500 mM NaCl and 20 mM imidazole). The crude cell lysate was loaded into a Ni-Sepharose HP column (XK 16/20) containing 10 ml resin equilibrated with binding buffer at flow rate of 1 ml/min. The column was eluted with the elution buffer (50 mM phosphate buffer pH 7.4, 500 mM NaCl and 500 mM imidazole). The eluted fractions with high lipase activity were subjected to SDS-PAGE and NATIVE-PAGE analysis to check the purity.

Lipase hydrolysis activity analysis and kinetic characterization

Lipolytic activity of ARM and R157S lipases were determined by measuring the amount of *p*-nitrophenol released after catalysis according to the method described by Winkler and Stuckman [13]. *p*-nitrophenyl laurate was used as the substrate in this study. The assay mixture contained 89µl of phosphate buffer (50 mM, pH 7), 10 µl of substrate solution (25 mM *p*-nitrophenol laurate in DMSO) and 1µl of enzyme solution. 100µl of ethanol was added after 15 second of the reaction time. The A_{410} of liberated p-nitrophenol was measured with *p*-nitrophenol as a standard [14]. The enzymatic *p*-nitrophenyl laurate hydrolysis was calculated by Hones-Woolf plot ([S]/v vs [S]). In this study, the concentration of enzymes [E_T] for ARM and R157S lipases was equal as constant. Thus, k_{cat} was calculated as equal to V_{max}. The k_{cat}, K_M, and k_{cat}/K_M were calculated for both ARM and R157S lipases and the results were compared. One unit of enzyme activity was defined as the rate of enzyme required releasing 1µmol of *p*-nitrophenol per minute from the *p*-nitrophenyl ester.

CD spectra

Thermodynamic stability of ARM and R157S lipases were obtained using a JASCO J-810 spectrapolarimeter (JASCO, Japan) and measured at 222 nm. 50 mM Phosphate buffer pH 7.0 was used as working buffer. CD spectra were recorded at temperature ranging from 20-90 °C using 0.1 cm path-length cuvettes. The concentration of ARM and R157S lipases were 0.4 mg/ml. All measurements were repeated three times.

Fluorescence spectra measurements

The fluorescence spectra were recorded using a Shimadzu RF-5301PC spectrofluorometer for intrinsic and extrinsic study of purified ARM and mutant lipases (0.001 mg/ml). An intrinsic fluorescence spectrum was recorded between 310 and 500 nm by excitation at 295 nm. The binding of a hydrophobic probe, 8-anilino-1-naphthalenesulfonate (ANS), to ARM and mutant lipases was determined as extrinsic study. ANS acts as a probe to determine changes in surface hydrophobic patches in a protein. Individual lipases in 50 mM phosphate buffer, pH 7.0, containing 100 mM NaCl and ANS solution (final concentration

Citation: Salleh AB, Abd Rahim ASM, Abdul Rahman RNZR, Leow TC, Basri M (2012) The Role of Arg157Ser in Improving the Compactness and Stability of ARM Lipase. J Comput Sci Syst Biol 5: 039-046. doi:10.4172/jcsb.1000088

10µM), were left at room temperature for 5 min. Fluorescence spectra were recorded between 400-600 nm upon exciting the protein at 350 nm to minimize the emission arising from Trp residues.

Results and Discussions

Modeling of ARM lipase and R157S lipase structures

The amino acid sequence of ARM lipase (accession number, ABK34427.1) was aligned with template sequence (2DSN) using available software packages; HOMOLOGY and MODELLER, Accelrys, San Diego. The unknown of ARM lipase structure (target protein) was built in a template of known 3D structure of T1 lipase (2DSN) with high similarity. The quality of predicted model structure is strongly dependent on the accuracy of the template structure used [15,16]. The predicted ARM lipase was determined using Ramachandran plot with 93.3% of residues being in the most favored regions. The percentage that higher than 90 % of residues in the most favored regions show that the quality of predicted structure is comparable to template [17]. Consensus approach was used as a method to substitute a critical residue with hot residue to increase the thermodynamic stability of ARM lipase. This technique was simple compared to other strategies [10,18]. The significant difference of Arg157 of ARM lipase and other thermostable lipases (Ser157) was targeted as a critical residue (Figure 1) and substituted using YASARA software. The energy minimization of ARM before mutation was -471 971.985 kJ/mol decrease to -507 569.663 kJ/mol after mutation as calculated using YASARA. The decreasing of minimized energy value of R157S showed that the substitution of Arg157 to Ser might contribute to a better compactness and increased the protein folding [19-21]. However, there was subtle change observed between ARM and R157S lipases as revealed by superimposed structures with RMSD value of 0.4804Å.

In Figure 2, Arg157 of ARM lipase showed high solvent accessible surface area (yellow surface) than Ser157 of mutant lipase inside the protein structure. The removal of Arg157 (less hydrophobic properties) inside the protein structure to Ser residue could increase the compactness and remove the bad cavities in the protein structure. For further analysis, VORONOIA has been used to study the packing of ARM and R157S lipases. The programme allows browsing of pre-calculated packing densities and cavities (http://bioinformatics.charite.de/voronoia.) [4]. From VORONOIA result (data not shown), the average packing density of R157S lipase increased and had lower internal cavities compared to the wild-type (ARM lipase). Thus, the substitution of bad residue (Arg157) with Ser enhanced the packing and compactness of the native structure besides decreasing the internal cavities in the protein structure.

Analysis of MD Simulations

Root Mean Square Deviation (RMSD)

Molecular Dynamic (MD) simulation techniques were used to analyze the dynamic behavior of the two lipases (ARM and R157S lipases). Trajectories over 10 ns were analyzed by calculating the RMSD of ARM and R157S lipases at 323K and 333K as shown in Figure 3. At the beginning of the trajectory (t=0), RMSD of both lipases displayed a value of 0.8Å indicated the movements of both lipases occurred during the thermalization and equilibration periods. At 323K, the deviation value of ARM lipase increased rapidly during the first 2 ns and maintained the deviation until the end of simulation (t=10 ns) (Figure 3A). Meanwhile, R157S lipase showed rapid increase of the deviation value (1.6 Å) until 8 ns and decreased to the end of simulation. R157S lipase structure was not stable and did not reach the folded state until end of the simulation at 50 °C. However, it is possible that at longer simulation times than 10 ns performed, the R157S lipase structure might be stable and reach at the folded state. MD simulation in long-time scale play an important role in increasing understanding of the dynamical aspects of protein structure. During longer time simulation, proteins continously fold and unfold and provide considerable insight into these process [23].

Different to the temperature at 333K (Figure 3B), the deviation of ARM lipase steadily increased until 2.0Å to 10 ns. In contrast, the deviation of R157S lipase was maintained at 1.3Å to the end of simulation (t=10 ns) and showed the R157S lipase had reached it folded state. The small peak at 1.8 ns explained that R157S lipase was tried to stabilize the structure. From these result, it showed that R157S lipase structure was stable and could maintain the conformation at 333 K (60°C), meanwhile ARM lipase could be stable at 323K/50°C. It is proven that the substitution of Arg157 with Ser had increased the thermal stability of protein structure in mutant lipase regarding to the longer stay in the folded state at higher temperature. Nosoh and Sekiguchi [22] state that the folded state of proteins is compact and rigid but become flexible because of vibrational and conformational entropy. However in the unfolded state, the polypeptide chain become less compact and more flexible. Xu et al. [25] examined partial coefficients of CL-20(001)/F_{2314} PBX at different temperatures and

```
                                                                121                                157          170
(EF042975l.1) Geobacillus sp. ARM lipase                        MLVSLLENGSQEEREYAKAHNVSLSPLFEGGHHFVLRVTTIATPHDGTTL  100%
(AF429311.1)  Bacillus stearothermophilus lipase                MLVSLLENGSQEEREYAKAHNVSLSPLFEGGHHFVLSVTTIATPHDGTTL   99%
(BA000043.1)  Geobacillus kaustophilus HTA426 lipase           MLVSLLENGSQEEREYAKAHNVSLSPLFEGGHHFVLSVTTIATPHDGTTL   97%
(AB457187.1)  Geobacillus sp. SBS-4s lipase                    MLVSLLENGSQEEREYAKAHNVSLSPLFEGGHHFVLSVTTIATPHDGTTL   94%
(AY149997.1)  Geobacillus thermoleovorans lipase              MLVSLLENGSQEEREYAKAHNVSLSPLFEGGHHFVLSVTTIATPHDGTTL   93%
(FJ640561.1)  Bacillus sp. L2 mutant lipase                    MLVSLLENGSQEEREYAKAHNVSLSPLFEGGHHFVLSVTTIATPHDGTTL   93%
(AF134840.1)  Bacillus thermoleovorans lipase                  MLVSLLENGSQEEREYAKAHNVSLSPLFEGGHHFVLSVTTIATPHDGTTL   92%
(AY855077.1)  Bacillus sp. L2 lipase                           MLVSLLENGSQEEREYAKAHNVSLSPLFEGGHHFVLSVTTIATPHDGTTL   92%
(AY787835.1)  Bacillus sp. 42 lipase                           MLVSLLENGSQEEREYAKAHNVSLSPLFEGGHHFVLSVTTIATPHDGTTL   92%
(AM396938.1)  Geobacillus thermoleovorans CCR11 lipase         MLVSLLENGSQEEREYAKAHNVSLSPLFEGGHHFVLSVTTIATPHDGTTL   92%
(AY260764.2)  Geobacillus zalihae T1 lipase                    MLVSLLENGSQEEREYAKAHNVSLSPLFEGGHHFVLSVTTIATPHDGTTL   91%
(AF141874.1)  Bacillus sp. TP10A.1 lipl lipase                 MLVSLLENGSKEEREYAKAHNVSLSPLFEGGHHFVLSVTTIATPHDGTTL   91%
(DQ009618.1)  Geobacillus sp. SF1 lipase                      MLVSLLENGSQEEREYAKEHNVSLSPLFEGGHRFVLSVTTIATPHDGTTL   90%
(DQ923401.1)  Geobacillus stearothermophilus s5 lipase         MLVSLLENGSQEEREYAKAHNVSLSPLFEGGHHFVLSVTTIATPHDGTTL   82%
                                                                **********:******* ******* *****.*** *************
```

Figure 1: Sequences alignment of ARM lipase and other homologous thermostable lipases from database through CLUSTALW multiple sequence alignment from Biology Workbench with percentage of identical to ARM lipase. The sequence alignment shows at positions 121 to position 170. The frame indicates at the position 157.

showed the increased of temperature from 248K to 348K decreased the activity of the modulus. The increasing of kinetic energy of the polymer molecules increased the comformational changes and the elasticity.

Root Mean Square Fluctuation (RMSF)

Root mean square fluctuation (RMSF) of each residue in ARM and R157S lipases was used to calculate over the trajectory for overall flexibility of the system at two different temperatures (323K and 333K). Figure 4A showed at 323K/50°C, a slight fluctuation was observed in ARM lipase with amino acid sequence of 130-145 which was at the flexible region of ARM lipase. The flexible region consists of α-helix and coil that was located in the surface of ARM lipase structure. The fluctuation of flexible region of ARM lipase then increased the flexibility at higher temperature (333K/60°C) as shown in Figure 4B. It was indicated that the flexible region was thermal sensitive region. The critical point mutation increased the protein folding and compactness due to less flexibility of flexible region.

Trajectories of MD simulations over 10 ns of ARM and R157S lipases structures were sampled at different temperature (50, 60 and 70°C) to analyze the differences of structural stabilities at different temperatures (Figure 5). The N-terminal of both lipases was quite mobile as shown in the structures before and after the simulations (10 ns) as expressed by different temperatures. The major fluctuation observed in the flexible regions consisting of α-helix structures showed by the arrow. The large fluctuation of flexible region would trigger an unfolding process and consequently denature the protein [25,27]. The conformational structure of ARM lipase and R157S lipase structures continuously change during the MD simulations at 50, 60 and 70°C until at the end of simulation (10 ns). Thus, in this study the conformational changes do not correlate to the thermal stability but better compactness and high rigidity are the major factors in protein thermal stability. R157S lipase had a compact and rigid protein structure due to its ability to remain stable and rigid at high temperature (60°C).

Solvent Accessible Surface Area (SASA)

Solvent accessible surface area of a protein that is accessible to a

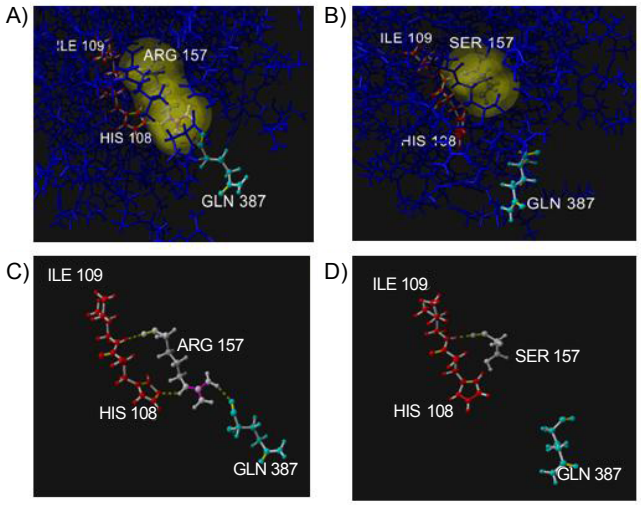

Figure 2: Modification introduced by the mutation. The solvent accessible surface area of the region around the residue Arg157 in ARM lipase (A) and Ser157 in R157S lipase (B). A detailed representation of H-bonds formation between Arg157 and Ser157 to the neighbour residues (C and D).

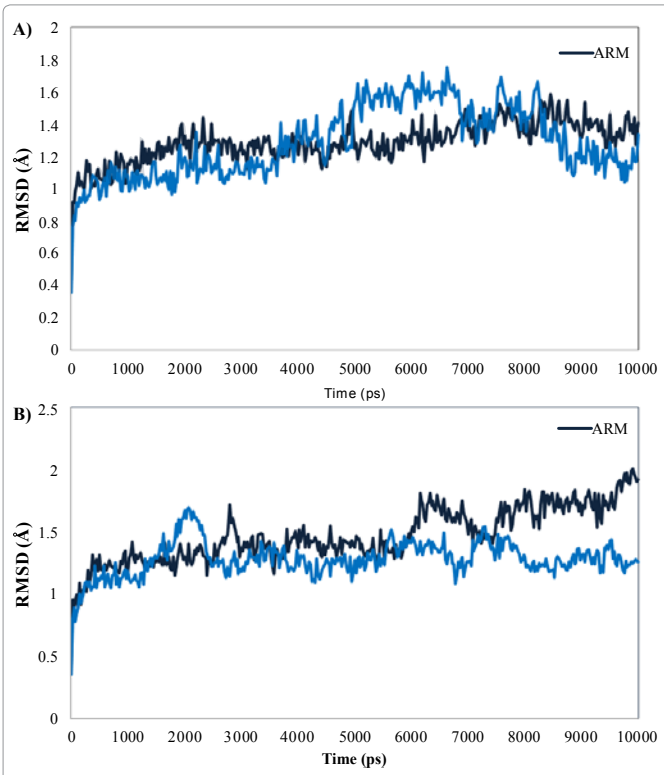

Figure 3: Root mean square deviation (RMSD) of the Cα position of ARM and R157S lipase backbone in (A) 323K/50°C and (B) 333K/60°C as obtained from the period of 0-10 ns.

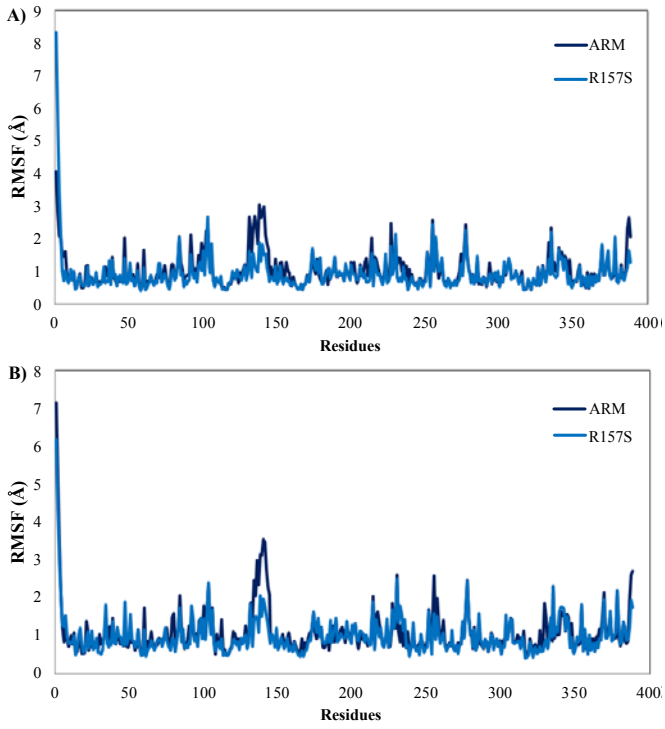

Figure 4: Root mean square fluctuations (RMSF) of the Cα position of ARM and R157S lipase backbone versus residue in different temperature (A) 323K/50°C and (B) 333K/60°C during 10ns simulations.

solvent and used to calculate the transfer of free energy that required moving a protein from aqueous solvent to a non-polar solvent such as lipid environment [22]. Figure 6 showed significant decreased in total solvent accessible surface value of R157S lipase (15,000 to 15,200 Å^2) at 323K/50°C and 333K/60°C than the wild-type lipase (15,400 to 16,000 Å^2) until the end of simulation (10 ns). Accessible surface areas of atoms are correlated with their hydrophobicities and folding process. Folding process is usually accompanied by the significant decrease in SASA value [28]. Therefore, the slightly decreased of SASA value in R157S lipase indicated that the mutant lipase structure was high in folding process. The replacement of polar residue, Arg (less hydrophobicity) with higher hydrophobicity residue, Ser increased the non polar residues located inside the protein structure could favour the protein packing and thus decreasing the internal cavities in the protein structure. Bisignano and Moran [24] reported that deletion of residue F508 increased SASA value of 73 Å^2 and led to local rearrangements that modify the energy interaction with the solvent.

Radius of Gyration (R_g)

Radius of gyration of ARM and R157S lipases were calculated with the conformations from the trajectories at 10 ns to get a global review that caused by different temperatures as shown in Figure 7. The radius of gyration of R157S lipase maintained vibration around 20.2 Å at 323K/50°C and 333K/60 °C. On the other hand, at low temperature (50°C), the radius of gyration of ARM lipase maintained around 20.3 Å (Figure 7A) and increased rapidly by time until 20.5 Å when the temperature increased to 60°C (Figure 7B). Thus, the mutant lipase could prevent its region in the structure from losing their native compactness at higher temperature (60°C). The hydrophobic stabilization is proportional to the reduction of surface area accessible to solvent on protein folding [22,29]. The critical point mutation has indirectly improved the hydrophobic interaction in native protein structure; possibly by rigidification of native structure resulting in improved core packing. Liu et al. [30] analyzed the thermal stability of 1V29 and 1UGQ and showed that the average radius of gyration of 1V29 decreased to 21.2Å below 350 K and exhibited higher compactness.

Preparation of purified ARM and mutant lipase

Based on the computational results, the substitution of bad residue

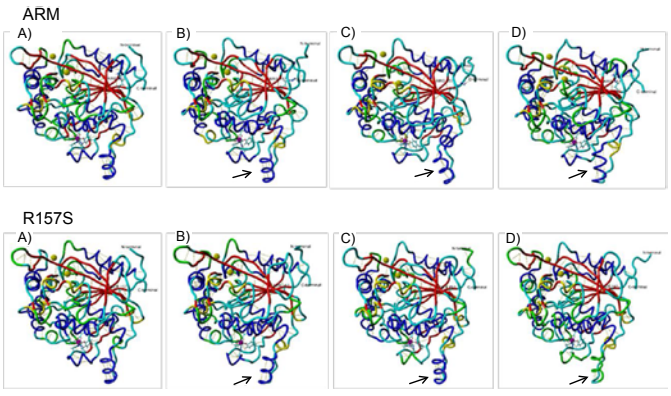

Figure 5: Graphic representation of ARM and R157S lipases 3D structure in 10ns simulation; A) control (0ns), B) 50 °C, C) 60 °C and D) 70 °C. The figures are colored by their secondary structure, where the red indicate β-sheets, blue represent α-helices, yellow represent 3_{10} helices, the loops are the green and the cyan segments are random coil. The residues of Arg/Ser 157, N- and C- termini are labeled. The arrows show position of flexible regions in the structure.

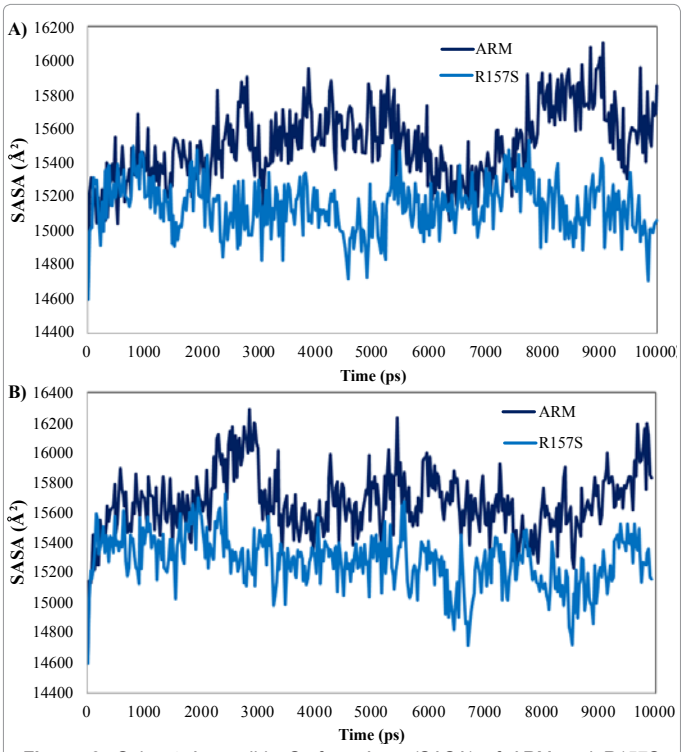

Figure 6: Solvent Accessible Surface Area (SASA) of ARM and R157S lipases at different temperature (A) 323K/50°C and (B) 333K/60°C during 10ns simulations.

(Arg157) contributed to the ARM lipase stability. Thus, site-directed mutagenesis was used to validate the computational results. The oligonucleotide primers containing the desired mutation (R157S) at the centre primer were used in the QuikChange Lightning Site-Directed Mutagenesis method. The successful mutant plasmid (R157S) was transformed into *E.coli* Top 10. Purification of ARM and R157S lipases had been conducted using AKTAprime ™ by one-step purification Nickel Sepharose affinity chromatography system. ARM and R157S lipases showed a single peak in the affinity purification profile. The purified ARM and R157S lipases were confirmed to be homogenous by a prominent single band on SDS-PAGE and NATIVE-PAGE (Figure 8).

Fluorescence analysis

The effect of critical point mutation was examined by measuring the conformational changes of ARM and R157S lipases using intrinsic Trp fluorescence and extrinsic ANS fluorescence (Figure 9). The fluorescence of lipases originated from Trp, Tyr and Phe residues (aromatic ring residues). However, only Trp could absorb the longest wavelength than Tyr and Phe. Intrinsic fluorescence parameter like intensity and wavelength maxima (λ_{max}) provide excellent means for studying structural dynamics and polarity of lipase [31-33]. ARM and R157S lipases contain eight Trp residues at positions 19, 30, 40, 60, 234, 255, 313 and 348.

The intrinsic fluorescence spectra of ARM and R157S lipases excited at 295 nm and showed the maximum intensities at 336 nm (Figure 9A). The result showed insignificant red-shift in emission maximum between ARM and R157S lipases indicated that the microenvironment of Trp residues was not changed in the hydrophobic environment of the protein core in aqueous buffer. The peak emission intensity of

R157S lipase was decreased by 1.5 fold than ARM lipase. The increased fluorescence intensity of ARM lipase might probably contribute to the perturbations in the local environment of Trp residues. It indicated that the Trp was shielded from bulk water but not located in the hydrophobic core of the lipases [33]. Amada et al. [34] stated that the red-shifting of *Pseudomonas sp*. MIS38 (PML) in the presence of 4 M GdnHCl exhibited at maximum intensity. It was probably because of the fully exposed aromatic residues to the solvent.

The effect of single point mutation was further supported by the fluorescence behaviour of ANS. ANS fluorescence spectra (extrinsic) of ARM and R157S lipases showed the highest intensity at 514 nm (Figure 9B). The peak emission intensity of R157S lipase was significantly decreased about 4-fold compared to ARM lipase. The decreasing of peak emission intensity suggesting decreased exposure of surface hydrophobic patches in the R157S lipase. Similar to *Bacillus subtilis* lipase LipA as reported by Rajakumara et al. [35], the ability of ANS to bind sharply in the native or unfolded lipase increased by 10-fold during heating lipase at 45°C. At the extreme temperature, there was a significant loss of secondary structure of lipase. Thus, the decreasing of ANS fluorescence intensity was significantly similar to the decreasing of intensity of Trp fluorescence and did not change the emission red-shift. It showed that the substitution of Arg157 to Ser has increased the compactness and protein folding.

Kinetic characterization

Kinetic parameters of ARM and R157S lipases were calculated to characterize the enzyme activity in the k_{cat}, K_M and k_{cat}/K_M values as a function of temperature (Figure 10). The behaviour of k_{cat} values (Vmax values used as concentration of enzymes were the same constant) measured within the studied temperature range 20-80 °C. R157S lipase showed the highest k_{cat} value of 55.5 sec^{-1} at 60 °C. Meanwhile, ARM lipase had k_{cat} value of 16.7 sec^{-1} at 50 °C. Bustos-Jaimes et al. [36] reported that the changes in k_{cat} value might be due to noticeable changes in K_M. The highest K_M value was 900 mM for ARM lipase at 50 °C. On the other hand, R157S lipase had K_M value of 700 mM at 60 °C. The K_M values decreased with temperature due to hydrophobic interactions that become stronger when the temperature increased [37]. Interestingly, both ARM and R157S lipases displayed high k_{cat}/K_M values at 70 °C due to low K_M values. R157S lipase showed k_{cat}/K_M values five times higher than ARM lipase. It explained that R157S lipase had essentially moved towards kinetic perfection with enhanced possibilities for productive substrate capture in the active site. The substitution of large and less hydrophobicity residue (Arg157) inside the protein structure increased hydrophobicity interaction and produced local flexibility and mobility of amino acids.

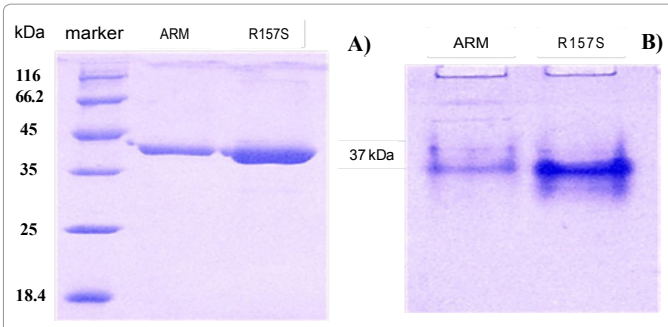

Figure 8: SDS-PAGE (A) and NATIVE-PAGE (B) of purified ARM and R157S lipases.

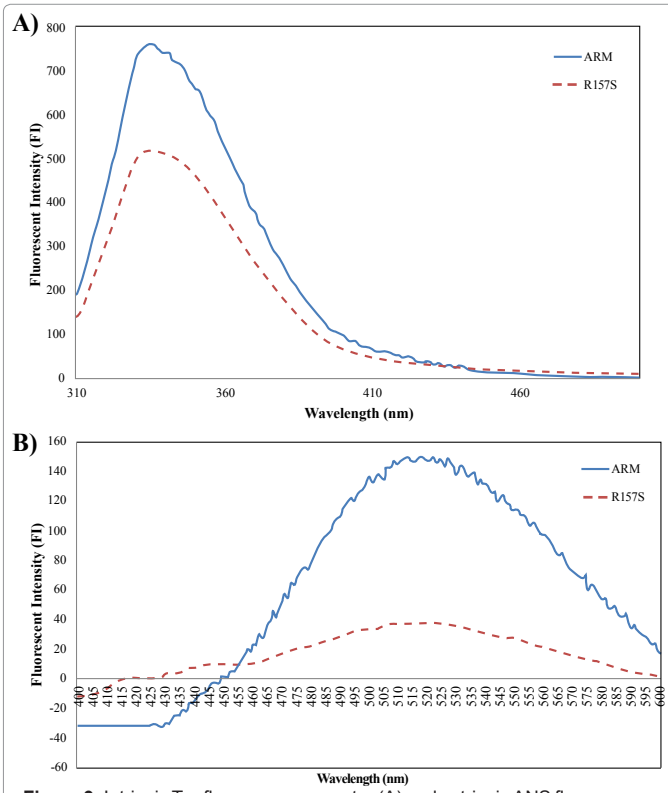

Figure 9: Intrinsic Trp fluorescence spectra (A) and extrinsic ANS fluorescence spectra (B) of ARM and R157S lipases.

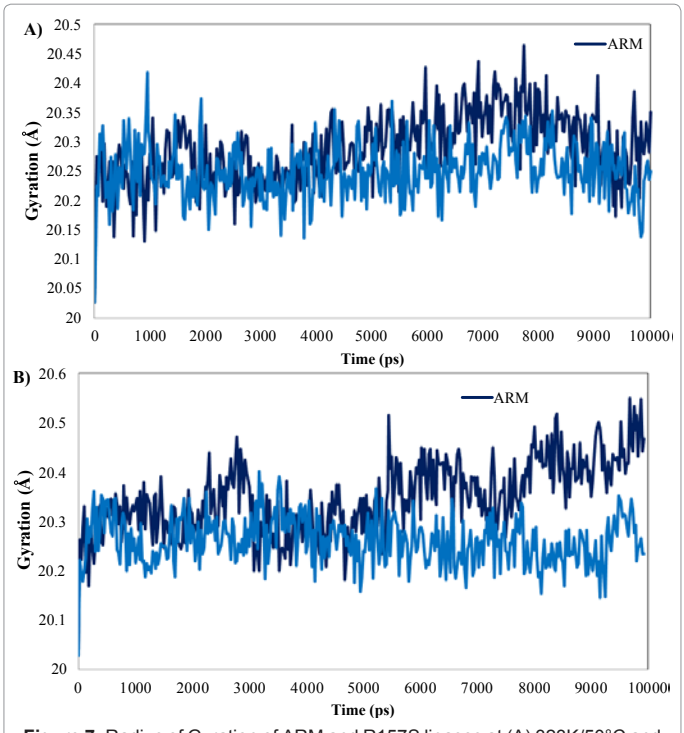

Figure 7: Radius of Gyration of ARM and R157S lipases at (A) 323K/50°C and (B) 333K/60°C during 10ns simulations.

Thermodynamic stability

CD spectroscopy was used to study the effect of critical point mutation towards thermodynamic stability. The CD spectra of the ARM and R157S lipases were measured at various temperatures (50-80°C) at 222 nm as shown in Figure 11. Ellipticity of ARM and R157S lipases at 222 nm increased by temperature. Upon heating from 60 to 70°C, the ellipticity of ARM lipase increased rapidly meanwhile R157S lipase increased the elipticity from 68 to 80°C. The thermal transition curve obtained by temperature dependence graph at 222 nm also supported that mutant lipase increased the thermostability.

The melting temperature (T_m) measured by CD is directly related to protein stability. R157S showed higher T_m value (71.6°C) than its wild-type (63.9°C) indicated that the mutant lipase increased its thermostability. As such, it was assumed that the substitution of less hydrophobic residue (Arg157) to more hydrophobic residue (Ser) increased the internal hydrophobicity of R157S lipase to maintain the structural stability at a high temperature. Choi et al. [38] reported that the wild-type enzyme which have Zn^{2+} elevated the T_m value from 51.1 to 69.3°C compared to its mutant enzymes (H87A, D61A/H87A and D61A/H81A/H87A/D238A). It indicated the importance of Zn^{2+} for maintaining structural stability at high temperature.

Conclusions

The choice of critical point mutation through consensus approach provides a very advantageous strategy of protein engineering. The substitution of Arg157 to Ser was made to increase the internal hydrophobicity of protein structure and protein folding. The MD simulations results (RMSD, RMSF, SASA, and radius of gyration) showed that R157S lipase had reached the folded state at 60°C and less flexible than ARM lipase (50°C). However, both lipases could not stand at extreme temperature (more than 70°C). Fluorescence study revealed that R157S lipase had increased in protein folding and compactness. Circular dichorism showed that R157S lipase increased protein stability and exhibited higher T_m value (71.6°C) than its wild-type (63.9°C). Kinetic study explained that R157S lipase had attained kinetic perfection and enhanced the possibilities for productive substrate capture in the active site. Further, the substitution of Arg157 (less hydrophobic) to Ser increased the internal hydrophobicity of the protein structure. Although Arg157 is polar and large side chain (guanidine group) to form high H-bond interactions than Ser, only the formation of large number of H-bonds could stabilize the protein structure. The compactness of R157S lipase was increased due to low cavities in the protein molecule. Both computational studies and biophysical analysis can be used together to engineer new protein and significantly contribute in understanding the relationship of protein and structure.

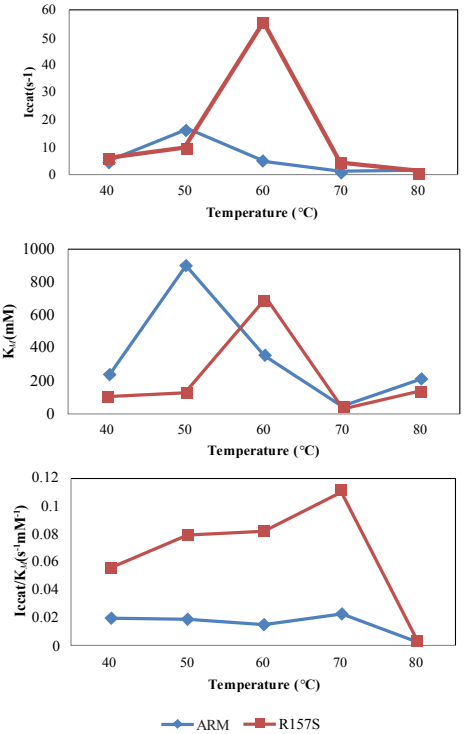

Figure 10: Temperature dependence on kinetic constants of ARM and R157S lipases A) k_{cat} B) K_M C) K_{cat}/K_M. Kinetic parameters were calculated from Hones-Woolf plot.

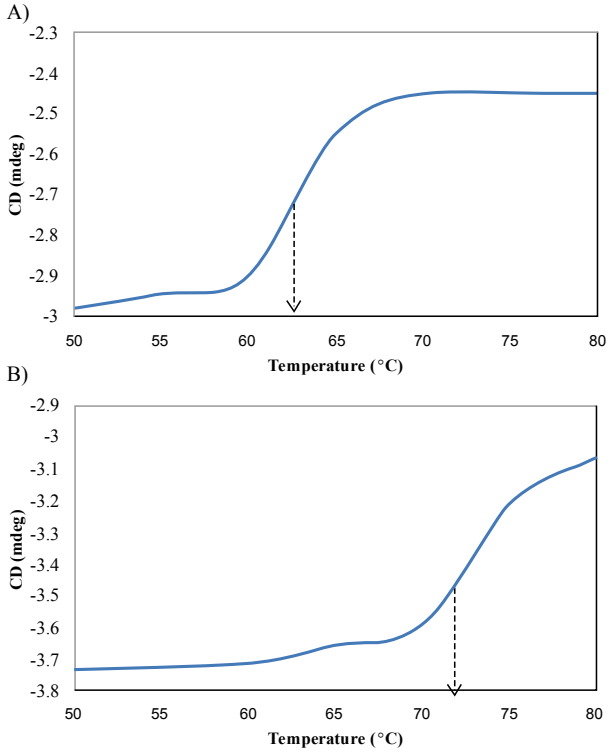

Figure 11: Temperature dependence of the CD (mdeg) at 222 nm for ARM (A) and R157S (B) lipases.

Authors' Contributions

ABS, RNZRAR, TCL and MB conceived the idea of the study, obtained the research grant, worked out the experimental design, analyzed and discussed the results with ASMAR. ASMAR performed the experiments described in this paper. ASMAR drafted the initial paper, and revised by all the authors. All authors read and approved the final manuscript.

Acknowledgements

The financial support by Research University Grants (RUGS) (91593) from Universiti Putra Malaysia is gratefully acknowledged.

References

1. Dandavate V, Jinjala J, Keharia H, Madamwar D (2009) Production, partial purification and characterization of organic solvent tolerant lipase from

Burkholderia multivorans V2 and its application for ester synthesis. Bioresour Technol 100: 3374-3381.

2. Bora L, Kalita MC (2007) Production and optimization of thermostable lipase from a thermophilic Bacillus sp LBN 4. The Internet Journal of Microbiology 4: 1.
3. Kumar S, Tsai CJ, Nussinov R (2000) Factors enhancing protein thermostability. Protein Eng 13: 179-191.
4. Rother K, Hildebrand PW, Goede A, Gruening B, Preissner R (2009) Voronoia: analyzing packing in protein structures. Nucleic Acids Res 37: 393-395.
5. Petsko GA, Ringe D (2004) Protein Structure and Function. New Science Press Ltd.
6. Fersht A (2002) Structure and Mechanism in Protein Science. A guide to enzyme catalysis and protein folding. Fourth pinting. W.H. Freeman and Company.
7. Cedrone F, Menez A, Quemeneur E (2000) Tailoring new enzyme functions by rational redesign. Curr Opin Struct Biol 10: 405-410.
8. Montanucci L, Foriselli P, Martelli PL, Casadio R (2008) Predicting protein thermostability changes from sequence upon multiple mutations. Bioinformatics 24: 190-195.
9. Toscano MD, Waycechoursky KJ, Hilvert D (2007) Minimalist active-site redesign: Teaching old enzymes new tricks. Angew Chem Int Ed Engl 46:3212-3236.
10. Arnold FH, Wintrode PL, Miyazaki K, Gershenson A (2001) How enzymes adapt: lessons from directed evolution. Trends Biochem Sci 26: 100-106.
11. Ebrahimpour A, Rahman RNZRA, Basri M, Salleh AB (2011) High level expression of a novel thermostable , organic solvent tolerant, 1,3-regioselective lipase from Geobacillus sp. Strain ARM. Bioresour Technol 102: 6972-6981.
12. Essmann U, Perera L, Berkowitz ML (1995) A smooth particle-mesh Ewald potential. Journal of Computational Physics 103: 5577-8592.
13. Winkler UK, Stuckmann M (1979) Glycogen, hyaluronate, and some other polysaccharides greatly enhance the formation of exolipase by Serratia marcescens. J Bacteriol 138: 663–670.
14. Zuo K, Zhang L, Yao H, Wang J (2010) Isolation and functional expression of a novel lipase gene isolated directly from oil-contaminated soil. Acta Biochim Pol 57:305-311.
15. Tramontano A (2006) Protein Structure Prediction: Concepts and Applications. WILEY-VCH Verlag GmbH & Co KGaA Weinheim.
16. Rodriguez R, Chinea G, Lopez N, Pons T, Vriend G (1998) Homology Modeling, model and software evaluation three related resources. Bioinformatics 14: 523-528.
17. Ramachandran GN, Ramakrishnan C, Sasisekharan V (1963) Stereochemistry of polypeptide chain configurations. J Mol Biol 7: 95-99.
18. Vieille C, Zeikus JG (2001) Hyperthermophilic enzymes: sources, uses, and molecular mechanisms for thermostability. Microbiol Mol Biol Rev 65: 1-43.
19. Guncheva M, Zhiryakova D (2011) Catalytic properties and potential applications of Bacillus lipases. Journal of Molecular Catalysis B: Enzymatic 68: 1-21.
20. Holtje HD, Sippl W, Rognan D, Folkers G (2008) Molecular Modeling: Basic Principles and Applications. WILEY-VCH Verlag GmbH & Co KGaA, Weinheim.
21. Tyndall JDA, Sinchaikul S, Fothergill-Gilmore LA, Taylor P, Walkinshaw MD (2002) Crystal Structure of a Thermostable Lipase from Bacillus stearothermophilus P1. J Mol Biol 323: 859–869.
22. Nosoh Y, Sekiguchi T (1991) Protein stability and stabilization through protein engineering. Ellis Horwood Limited.
23. Klepeis JL, Lindorff-Larsen K, Dror RO, Shaw DE (2009) Long-timescale molecular dynamics simulations of protein structure and function. Curr Opin Struct Biol 19: 120-127.
24. Bisignano P, Moran O, (2010) Molecular dynamics analysis of the wild type and dF508 mutant structures of the human CFTR–nucleotide binding domain 1. Biochimie 92: 51-57.
25. Xu X, Xiao J, Huang H, Li J, Xiao H (2010) Molecular dynamic simulations on the structures and properties of-CL-20(0 0 1)/F_{2314} PBX. J Hazard Mater 175: 423-428.
26. Kukol A (2008) Molecular Modeling of Proteins. Humana Press. Springer Science.
27. Kamal MZ, Ahmad S, Yedavalli P, Rao NM (2010) Stability curves of laboratory evolved thermostable mutants of a Bacillus subtilis lipase. Biochim Biophys Acta 1804: 1850–1856.
28. Richmond TJ (1984) Solvent accessible surface-area and excluded volume in proteins-analytical equations for overlapping spheres and implications for the hydrophobic effect. J Mol Biol 178: 63-89.
29. Tatsis VA, Stavrakoudis A, Demetropoulos IN (2008) Molecular Dynamics as a pattern recognition tool: An automated process detects peptides that preserve the 3D arrangement of Trypsin's Active Site. Biophys Chem 133: 36-44.
30. Liu J, Yu H, Shen Z (2008) Insights into thermal stability of thermophilic nitrile hydratases by molecular dynamic simulation. J Mol Graph Model 27: 529-535.
31. Ahmad E, Fatima S, Khan MM, Khan RH (2010) More stable structure of wheat germ lipase at low pH than its native state. Biochimie 92: 885-893.
32. Angkawidjaja C, Matsumura H, Koga Y, Takano K, Kanaya S (2010) X-ray Crystallographic and MD simulations studies on the mechanism of interfacial activation of a family 1.3 lipase with two lids. J Mol Biol 400: 82-95.
33. Kwaambwa HM, Maikokera R (2007) A fluorescence spectroscopic study of coagulating protein extracted from Moringa oleifera seeds. Colloids Surf B Biointerfaces 60: 213-220.
34. Amada K, Kwon HJ, Haruki M, Morikawa M, Kanava S (2001) Ca(2+) -induced folding of a family 1.3 lipase with repetitive Ca(2+) binding motifs at the C-terminus. FEBS Lett 509: 17-21.
35. Rajakumara E, Acharya P, Ahmad S, Sankaranaryanan R, Rao NM (2008) Structural basis for the remarkable stability of Bacillus subtilis lipase (Lip A) at low pH. Biochim Biophys Acta 1784: 302–311.
36. Bustos-Jaimes I, Mora-Lugo R, Calcagno ML, Farrés A (2010) Kinetic studies of Gly28: Ser mutant form of Bacillus pumilus lipase: Changes in kcat and thermal dependence. Biochim Biophys Acta 1804: 2222–2227.
37. Chandler D (2005) Interfaces and the driving force of hydrophobic assembly. Nature 437: 640–647.
38. Choi WC, Kim MH, Ro HS, Ryu SR, Oh TK, et al. (2005) Zinc in lipase L1 from Geobacillus stearothermophilus L1 and structural implications on thermal stability, FEBS Lett 579: 3461–3466.